



<b>Customer:</b> ESA	<b>Document Ref:</b> OMPC.ACR.MEM.41
<b>Contract No.:</b> 4000136252/21/I-BG	<b>Date:</b> 01/08/2025
	<b>Issue:</b> 1.0

<b>Project:</b>	COPERNICUS SPACE COMPONENT SENTINEL OPTICAL IMAGING MISSION PERFORMANCE CLUSTER SERVICE
<b>Title:</b>	RUT error sources analysis
<b>Author(s):</b>	Alexis Deru, Sebastien Clerc, Emmanuel Hillairet, Bruno Lafrance, Rémi Bellouard
<b>Distribution:</b>	ESA
<b>Filename</b>	OMPC.ACR.MEM.41 - i1r0 - RUT Error sources analysis.docx

**Copyright ©2024 – ACRI-ST**  
*All rights reserved.*

*No part of this work may be disclosed to any third party translated, reproduced, copied or disseminated in any form or by any means except as defined in the contract or with the written permission of ACRI-ST*

**ACRI-ST**  
**260 route du Pin Montard**  
**06904 Sophia-Antipolis, France**  
**Tel: +33 (0)4 92 96 75 00 Fax: +33 (0)4 92 96 71 17**  
**[www.acri-st.fr](http://www.acri-st.fr)**

**Disclaimer**

The views expressed herein can in no way be taken to reflect the official opinion of the European Space Agency or the European Union



### Changes Log

Version	Date	Changes
1.0	01/08/2025	Creation of the document

### List of Changes


Version	Section	Answers to RID	Changes

## Table of content

<b>1</b>	<b>INTRODUCTION .....</b>	<b>1</b>
1.1	SCOPE OF THE DOCUMENT .....	1
1.2	METROLOGY FRAMEWORK .....	1
1.3	EFFECTS TABLE .....	2
<b>2</b>	<b>NOISE MODEL .....</b>	<b>4</b>
2.1	MODEL.....	4
2.2	ESTIMATION .....	4
2.3	MODEL COMPARISON .....	5
2.4	SYNTHESIS AND WAY FORWARD .....	6
2.5	CORRELATIONS.....	6
<b>3</b>	<b>NON-LINEARITY .....</b>	<b>7</b>
3.1	IMPACT ANALYSIS .....	7
3.2	SYNTHESIS AND WAY FORWARD .....	7
3.3	CORRELATIONS.....	8
<b>4</b>	<b>STRAYLIGHT .....</b>	<b>9</b>
4.1	IN-THE FIELD STRAYLIGHT.....	9
4.1.1	<i>Mission requirement</i> .....	9
4.1.2	<i>Assessment on Moon images</i> .....	10
4.1.3	<i>Synthesis and way forward</i> .....	11
4.2	OUT-OF-FIELD STRAYLIGHT .....	12
4.2.1	<i>Impact analysis</i> .....	12
4.2.2	<i>Model</i> .....	13
4.2.3	<i>Synthesis and way forward</i> .....	13
4.3	CORRELATION .....	13
<b>5</b>	<b>ELECTRONIC CROSS-TALK .....</b>	<b>14</b>
5.1	STANDARD (LINEAR) CROSS-TALK.....	14
5.1.1	<i>Description and correction</i> .....	14
5.1.2	<i>Correction residual</i> .....	15
5.2	OTHER CROSS-TALK EFFECTS.....	15
<b>6</b>	<b>POLARIZATION SENSITIVITY .....</b>	<b>17</b>
6.1	IMPACT ANALYSIS .....	17
6.2	SYNTHESIS AND WAY FORWARD .....	18
6.3	CORRELATIONS.....	18
<b>7</b>	<b>ON-BOARD COMPRESSION NOISE.....</b>	<b>19</b>
7.1	DESCRIPTION .....	19
7.2	IMPACT ANALYSIS .....	19
7.2.1	<i>Flattening</i> .....	19
7.2.2	<i>Butterflies</i> .....	20
7.2.3	<i>Order of magnitude</i> .....	20

7.3	POSSIBLE MODELLING APPROACHES .....	20
7.3.1	<i>Detection of flattening in the signal of blind pixels</i> .....	20
7.3.2	<i>Monitoring of truncation level during decompression</i> .....	21
7.4	SYNTHESIS AND WAY FORWARD .....	21
7.5	CORRELATION .....	21
<b>8</b>	<b>SPECTRAL RESPONSE KNOWLEDGE .....</b>	<b>22</b>
8.1	DESCRIPTION .....	22
8.2	IMPACT ANALYSIS .....	25
8.3	WAY FORWARD .....	28
8.4	CORRELATION .....	28
<b>9</b>	<b>RADIOMETRIC CALIBRATION UNCERTAINTY .....</b>	<b>29</b>
9.1	DESCRIPTION .....	29
9.1.1	<i>Gains</i> .....	29
9.1.2	<i>Offsets</i> .....	29
9.2	MODELLING .....	30
9.3	SYNTHESIS AND WAY FORWARD .....	31
9.4	CORRELATION .....	31
<b>10</b>	<b>ORTHORECTIFICATION: NOISE FILTERING .....</b>	<b>33</b>
10.1	DESCRIPTION .....	33
10.2	MODELLING .....	33
10.3	WAY FORWARD .....	33
10.4	CORRELATION .....	34
<b>11</b>	<b>ORTHORECTIFICATION: RESAMPLING ERROR .....</b>	<b>35</b>
11.1	DESCRIPTION .....	35
11.2	MODELLING .....	35
11.3	WAY FORWARD .....	36
11.4	CORRELATION .....	36
<b>12</b>	<b>GEOMETRIC UNCERTAINTY .....</b>	<b>37</b>
12.1	DESCRIPTION AND IMPACT ANALYSIS .....	37
12.2	MODELLING .....	37
12.3	WAY FORWARD .....	37
12.4	CORRELATION .....	37
<b>13</b>	<b>L1C IMAGE QUANTIZATION AND COMPRESSION ERROR .....</b>	<b>38</b>
13.1	DESCRIPTION AND IMPACT ANALYSIS .....	38
13.2	SYNTHESIS AND WAY FORWARD .....	38
<b>14</b>	<b>CONCLUSIONS .....</b>	<b>39</b>
<b>15</b>	<b>REFERENCES .....</b>	<b>40</b>



	<p><b>OPT-MPC</b></p> <p><b>RUT error sources analysis</b></p>	<p>Ref.: OMPC.ACR.MEM.41  Issue: 1.0  Date: 01/08/2025  Page: 1</p>
--	--	---

# 1 Introduction

## 1.1 Scope of the document

This document provides an analysis of the error sources to be considered for the Sentinel-2 Level-1C Radiometric Uncertainty Tool.

For each error source, we discuss:

- Its origin
- Its qualitative and quantitative impact, and in which cases the error source can be neglected
- Possible modeling approaches.

This document serves a design justification for the L1C RUT and input to the ATBD.


## 1.2 Metrology framework

The GUM [RD9] provides the general framework to deal with measurement uncertainty. Its application to Earth Observation measurements is rendered difficult by several aspects:

- Traceability to SI cannot be enforced post-launch, and environmental effects cannot easily be characterized. Therefore, the uncertainty analysis will have to rely on assumptions or empirical estimations regarding ageing and other environmental effects.
- Repeated measurements of a measurand (either using the same or different sensors) is a cornerstone of metrology. This is however generally not possible in Earth Observation as observation conditions vary rapidly.
- EO provides a massive amount of measurements in the spatial, temporal and spectral dimensions. These measurements are often combined by downstream users to extract useful information (multi-spectral processing, spatio-temporal aggregation, etc.) The error sources affecting these measurements have various levels of correlation, which need to be taken into account for uncertainty propagation in downstream data products.

To cope with these issues, we have made a number of choices:

- When effects could not be fully characterized on-ground, we used assessment based on analysis of EO images. In cases where this was not possible, the error sources remain not modelled, even though they may not be fully negligible.
- In the general metrology context, the uncertainty characterizes the expected dispersion of the error for repeated measurements of the same quantity. In the EO context it describes the expected distribution of errors over all pixels of the image. As a result, error sources affecting only a few pixels can be neglected.

	<p><b>OPT-MPC</b></p> <p><b>RUT error sources analysis</b></p>	<p>Ref.: OMPC.ACR.MEM.41  Issue: 1.0  Date: 01/08/2025  Page: 2</p>
--	--	---

- A full estimation of the correlations of error sources across measurements is out of scope at this stage. We can just provide, for each error source, an indication of the expected qualitative level of correlation across the spatial, temporal and spectral dimensions, as well as across satellite units. This is expected to help users understand if a given component should be considered for error propagation. For example, when computing a band ratio, one should consider that the geolocation error is highly correlated between spectral bands ; the contributions for each band should therefore not be added quadratically.

An important aspect of the metrology framework concerns the precise definition of the measurand. Indeed, all measurement errors are defined with the respect to a given measurand. For the S2 RUT, the L1C measurand is the directional top-of-atmosphere reflectance for a given pixel and spectral band, assuming:

- The pixel value corresponds to the integrated signal for the satellite Point-Spread-Function (PSF, as provided in the on-line documentation). The deviation of the PSF from an ideal rectangle is not considered as an error source.
- The spectral response for each spectral band is described in the product metadata (also available in the on-line documentation). The spectral response functions are slightly different for each satellite unit, so the measurands are also slightly different.
- An approximate sensing time stamp is provided at tile level. The actual sensing time depends on the pixel and spectral band (typically within  $\pm 15$  seconds of the tile sensing time).
- Illumination and viewing angles are provided on a coarse grid and can be interpolated with a reasonable accuracy for each pixel and spectral band. Reflectances are computed with respect to the reference ellipsoid.


Finally, we mention that the out-of-field straylight term required a specific treatment. Indeed this effect is expected to introduce a systematic positive error. According to the GUM, such systematic errors should be corrected to the best available knowledge, and only correction residuals should be considered in the uncertainty budget. However such a straylight correction is not practical in L1 processing due to a lack of knowledge on its value. Indeed, the out-of-field straylight was only coarsely characterized on ground. More fundamentally, a correction would require a knowledge of light sources outside of the field of view. Using a coarse correction would probably result in a degradation of the image quality in most cases, including the introduction of unphysical negative reflectances. Following the approach in [RD1] (see also [RD9] part 3, section 6.3.1 p. 14), we add this estimated error linearly to the uncertainty budget.

### 1.3 Effects table

The following table summarizes the list of effects affecting radiometric measurements and documents its status in the RUT V1 and expected correlations of the errors across-measurements.

**Table 1: Effects table.**

		Correlation				
	Source	Status RUT V1	temporal	spatial	spectral	inter-satellite
<b>L1B</b>	Instrument noise (incl. quantization, dark noise)	modelled	no	no	no	no
	in-the field straylight	not modelled	partially	locally	partially	yes
	Out of field straylight	modelled	no	partially	partially	yes
	cross-talk correction residual error	negligible				
	polarization sensitivity	not modelled	no	locally	yes	yes
	on-board compression noise	not modelled	no	locally	no	no
	dark signal correction residual error	negligible				
	non-linearity correction residual error	modelled	partially	no	no	no
	spectral response non-uniformity	not modelled	yes	partially	no	no
	L1B image quantization	negligible				
	Radiometric calibration error	modelled	partially	partially	partially	partially
<b>L1C</b>	solar irradiance model error	negligible				
	Sun-satellite distance error	negligible				
	Cosine error	negligible				
	Orthorectification noise reduction	modelled				
	orthorectification interpolation error	not modelled	yes	locally	partially	yes
	Geolocation error	modelled	no	locally	partially	no
	L1C image quantization	negligible				

	<p><b>OPT-MPC</b></p> <p><b>RUT error sources analysis</b></p>	<p>Ref.: OMPC.ACR.MEM.41  Issue: 1.0  Date: 01/08/2025  Page: 4</p>
--	--	---

## 2 Noise model

### 2.1 Model

Measurements are affected by a random noise coming from:

- Quantum « shot » noise which follows the standard Poisson law whose standard uncertainty is equal to the square root of the measurement
- Electronic read out noise
- Quantization noise

The noise is considered as random, uncorrelated in the spectral, temporal and spatial domains.

The noise model takes the form:

$$\sigma_Z = \sqrt{\alpha^2 + \beta Z},$$

Where:

- $\alpha$  and  $\beta$  are the parameters of the model;
- $Z$  is the measured radiance signal expressed in Digital Counts (after dark signal subtraction and calibration)
- $\sigma$  is the noise standard deviation in Digital Counts.

The parameter  $\beta$  accounts for the shot noise, while  $\alpha$  accounts for the read out and quantization noise. When binning is applied to a spectral band measurement, the noise shall be scaled accordingly.

The model relies on the assumption that the noise level remains constant over time. Noise level monitoring results show that this assumption is valid for non-defective pixels.

### 2.2 Estimation

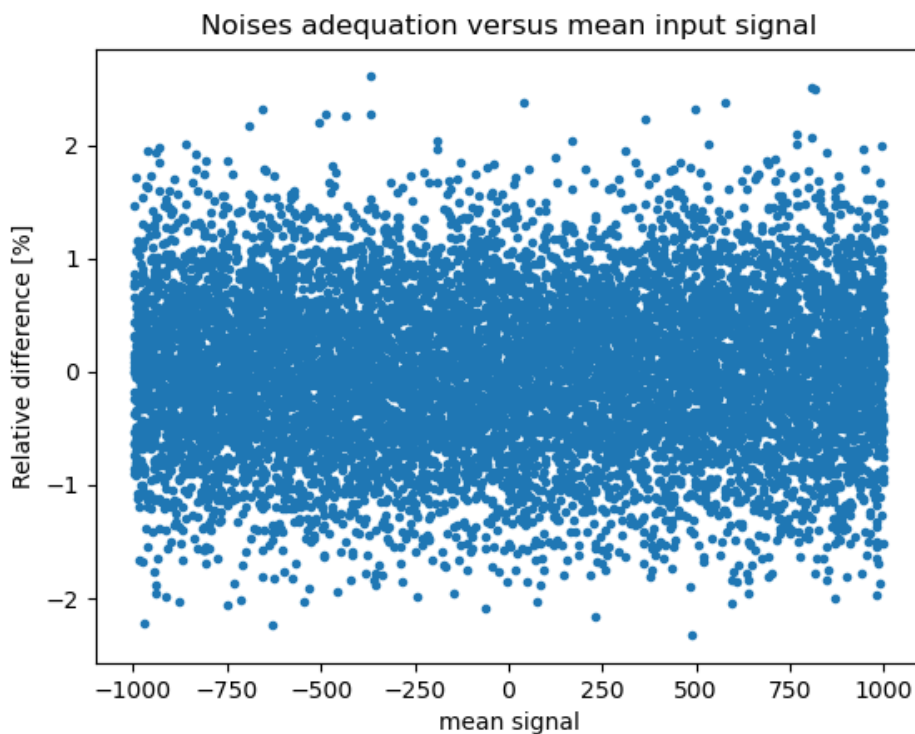
Four different approaches are possible:

- Estimation from detector characteristics (gain, detector read out noise and quantization noise, binning)
- Model fitting using Sun and Dark calibration images: parameter  $\alpha$  is determined from dark calibration images, and  $\beta$  from Sun calibration images at  $Z(Ldiff)$ . This approach is routinely applied by the MPC using the QCC software.
- Model fitting using Sun calibration images acquired at different integration times, and therefore different values of  $Z$ . This approach requires specific diffuser acquisitions. It was used by CNES during S2A and S2B commissioning.
- Model fitting using Earth Observation images: the noise variance is measured at different values of  $Z$  and a linear regression is applied to get the model parameters.

A dedicated test has been conducted regarding the quantisation noise contribution, in case of estimation through model fitting. The goal was to verify that the quantisation impact was still representative when using low radiance uniform images and to confirm that the resulting noise model includes a relevant quantisation contributor.

The measured noise level over a quantised sinusoidal signal is confirmed to be aligned with the theoretical noise level independently of the signal level itself. Samples of quantized sinusoidal signal with random mean level, amplitude and white noise level has been generated, then the noise level is measured with RMS between input signal and noisy-quantized one. The RMS is finally compared to the theoretical noise level.

The figure below presents the relative difference between the measured and theoretical noise levels in function of the mean input signal and shows that the adequation of the 2 noises estimation is not correlated to the signal level.



### 2.3 Model comparison

The figure below shows the comparison of the three different approaches described in the previous section for some spectral bands. It can be seen that the QCC and DLR models agree within 20%, while the CNES model behaves quite differently. The main differences between the QCC and DLR are observed on the atmospheric bands, which may reflect the lower accuracy of the L1B-based SNR estimation method on those bands. The accuracy of the fit based on L1B images is limited by the range of radiances in the test images. Although the QCC and DLR model

agree very well on intermediate values of radiances (close to  $L_{ref}$ ), the agreement is less good at very low or very high radiances.

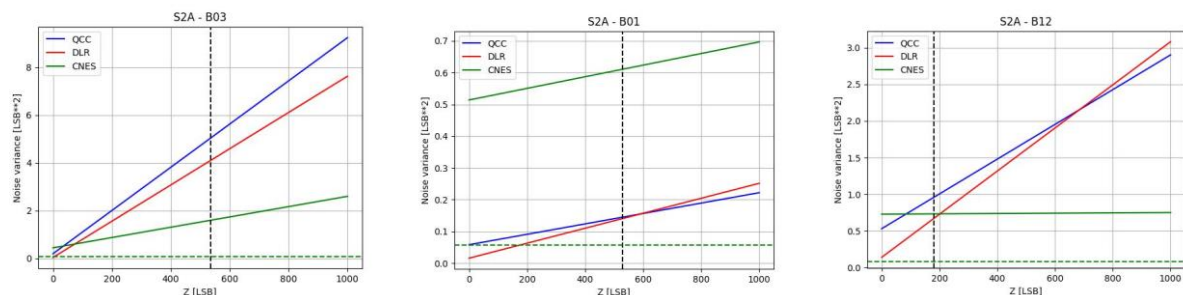


**Figure 1: Comparison of noise variance models: QCC (blue), DLR (red) and CNES (green). The vertical line indicates the value of the reference radiance  $L_{ref}$  (in LSB).**

## 2.4 Synthesis and way forward

For the RUT V1, we decide to use the QCC noise model. As of January 2025, the parameters of the QCC noise model are available in the L1C product metadata. For products generated before that date, the RUT can use a default configuration which provides average measured parameters for S2A, S2B and S2C. The temporal stability of the model is such that this value can be used at any time during the mission.

## 2.5 Correlations

The instrument noise is purely random, without any correlations.

## 3 Non-linearity

### 3.1 Impact analysis

The pixel response linearity is modelled using cubic (VNIR) or piecewise linear (SWIR) functions. Only the residual error needs to be considered in the uncertainty analysis.

For MSI A and B [RD6 and 7] the non-linearity residual was considered to be lower than 0.4% for all spectral bands.

For models C and D [RD8] a more detailed analysis was performed, considering various contributors to the non-linearity residual, including model fitting residual, characterization errors, etc. The analysis also considered the impact at different radiance levels (Lmin, Lref, Lmax), as well as typical (see table below) and worst-cases. The main outcomes from this study are:

- A typical error of 0.4% is confirmed for VNIR bands at Lref.
- The error is closer to 0.6% for bands B09 to B12, also at Lref.
- The relative error increases significantly at Lmin. However, in absolute terms it is expected to remain negligible with respect to other terms (noise, straylight, etc).
- Worst-case estimates are 0.6% for VNIR bands, and around 0.8% for B09 to B12. This concerns very few pixels.

*Table 2: Non-linearity residual error estimates for models C and D, typical case, from [RD8].*

	B1	B2	B3	B4	B5	B6	B7
@Lmin	0.85%	1.32%	2.42%	3.27%	3.30%	4.70%	6.02%
@Lref	0.40%	0.41%	0.41%	0.41%	0.41%	0.42%	0.43%
% of Lref where spec is met	12%	14%	16%	16%	15%	18%	19%


  

	B8	B8a	B9	B10	B11	B12
@Lmin	7.31%	8.40%	10.50%	13.90%	8.90%	33.08%
@Lref	0.41%	0.43%	0.78%	0.63%	0.65%	0.59%
% of Lref where spec is met	17%	22%	74%	55%	58%	53%

### 3.2 Synthesis and way forward

We propose to consider a constant relative error term:

- 0.4% for bands B01 to B8A
- 0.6% for bands B09 to B12

 <p><b>OPT-MPC</b> Copernicus Sentinel Optical Mission Performance Cluster</p>	<p><b>OPT-MPC</b></p> <p><b>RUT error sources analysis</b></p>	<p>Ref.: OMPC.ACR.MEM.41 Issue: 1.0 Date: 01/08/2025 Page: 8</p>
--	--	--

### 3.3 Correlations

---

The non-linearity error depends on the signal level and the pixel index. It is possible to assume no correlation between different pixels and between the same pixel for different satellite units. However, if the radiance level remains nearly constant over time, the error for a given L1C pixel may be partially correlated.

## 4 Straylight

### 4.1 In-the field straylight

#### 4.1.1 Mission requirement

A requirement exists for in the in-field straylight, and the effect in % of  $L_{ref}$ , at specific distances of a cloud at  $L_{cloud}$  radiance.

ID		Requirement
<p><b>DG-MSI-640</b></p> <p><b>MSI-640</b></p> <p><b>MSI-SA-115</b></p>	T,A	<p><i>Considering:</i></p> <p>a) An image composed of two uniform parts of infinite size and of different radiance; the radiance in one part is the “cloud” radiance <math>L_{cl}</math>, the radiance of the other part is comprised between the specified minimum and maximum radiances,</p> <p>b) The two parts are separated by a column or a row,</p> <p>The straylight level shall be less than or equal to 0.5% of <math>L_{ref}</math> at any distance from 300 metres to 1000 metres from the boundary column/row and shall be less than or equal to 0.1% of <math>L_{ref}</math> at any</p>

Ground tests performed on MSI S2A (PFM) and S2B (FM2) showed that the requirement of 0.1% of  $L_{ref}$  at 1 km of a cloud is not fully respected, see table below.

**Table 3: Ghost level measured at various distances for PFM and FM2 models, from [RD8]**

PFM			B1	B2	B3	B4	B5	B6	B7	B8	B8A	B9	B10	B11	B12
Cloud scene @ 300m	PFM ACT @ 300m	% Lref	0,9	1,6	1,5	1,0	0,6	0,7	1,0	0,2	0,5	5,1			
	PFM ALT @ 300m	% Lref	1,2	1,2	1,4	1,4	1,7	1,7	1,7	0,8	1,9	10,5			
Cloud scene @ 650m	PFM ACT @ 650m	% Lref	0,4	1,0	0,8	0,5	0,3	0,3	0,5	0,2	0,2	2,9	1,6	3,0	3,2
	PFM ALT @ 650m	% Lref	0,6	0,5	0,6	0,5	0,7	0,7	0,7	0,3	0,7	4,1	2,5	4,4	4,8
Cloud scene @ 1000m	PFM ACT @ 1000m	% Lref	0,3	0,6	0,6	0,4	0,2	0,2	0,3	0,2	0,2	1,8	0,9	1,5	2,0
	PFM ALT @ 1000m	% Lref	0,2	0,1	0,1	0,1	0,2	0,2	0,1	0,1	0,1	0,6	1	1,9	2,0
FM2			B1	B2	B3	B4	B5	B6	B7	B8	B8A	B9	B10	B11	B12
Cloud scene @ 300m	FM2 ACT @ 300m	% Lref	1,3	1,9	1,7	1,4	1,7	1,2	1,3	0,2	0,8	5,1			
	FM2 ALT @ 300m	% Lref	0,9	1,1	1,2	1,1	1,2	1,1	1,1	0,7	1,6	11,2			
Cloud scene @ 650m	FM2 ACT @ 650m	% Lref	0,5	1,1	0,8	0,7	0,4	0,3	0,6	0,1	0,2	1,8	1,2	2,1	1,6
	FM2 ALT @ 650m	% Lref	0,4	0,3	0,3	0,3	0,5	0,3	0,3	0,2	0,7	6,2	1,7	3,7	5,2
Cloud scene @ 1000m	FM2 ACT @ 1000m	% Lref	0,4	0,8	0,6	0,6	0,2	0,2	0,4	0,1	0,1	1,4	0,6	1,0	0,9
	FM2 ALT @ 1000m	% Lref	0,1	0,0	0,0	0,0	0,0	0,0	0,0	0,0	0,1	0,2	1,0	1,8	2,5

#### 4.1.2 Assessment on Moon images

On the other hand, the acquisition of the Moon for S2C provides the opportunity to analyse the behaviour of the halo (local straylight) visible around the Moon.

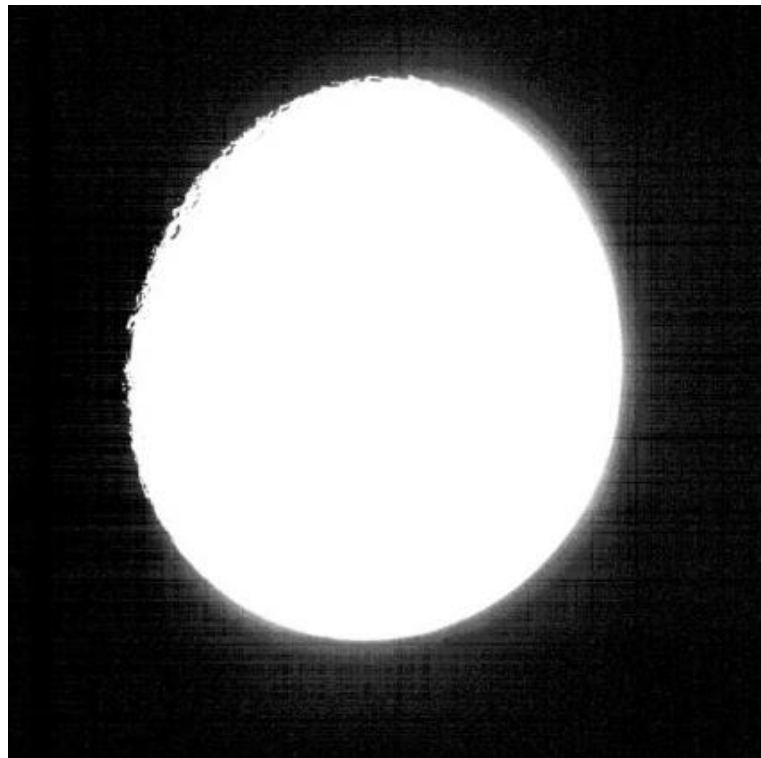


**Figure 2: S2C B02 Moon acquisition with Halo. radiometric stretch [0-10] LSB**

Once this phenomenon is considered straylight, it is proportional to the radiance of the source, and even if the Moon has a radiance much lower than the clouds (in the different spectral bands), the straylight could be evaluated, at different distances of the Moon, as a proportion of the radiance of the source.

For these computations, a radial profile is computed from the quarter of the Moon Disk providing the sharpest edge (depending on Sun orientation). ACL and ALT are mixed, considering symmetrical behaviour (which seems to be visually the case). This is to reduce the noise and quantization effect by averaging on a large number of samples.

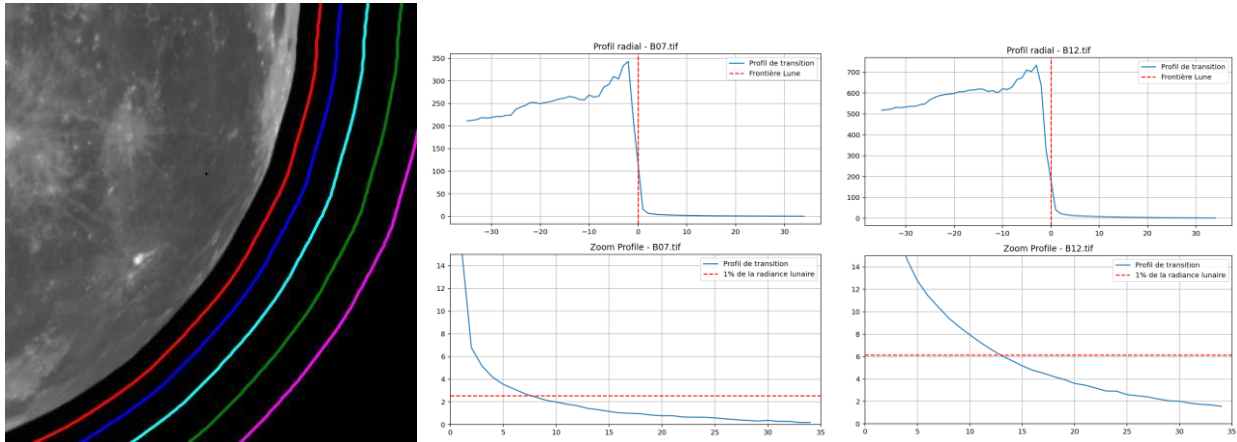


**Figure 3: estimation of straylight from halo profile around the Moon acquisition of December.**

**Table 4: estimation of % of straylight at different distances from the source.**

Band	% @ 150m	% @ 300m	% @ 500m	% @ 750m	% @ 1000m
B01.tif	1.196%	0.6279%	0.532%	0.2448%	0.1695%
B02.tif	1.208%	0.7578%	0.4471%	0.3288%	0.2489%
B03.tif	1.196%	0.6864%	0.4028%	0.1891%	0.126%
B04.tif	1.343%	0.7621%	0.3892%	0.2902%	0.213%
B05.tif	1.432%	0.6993%	0.3818%	0.2447%	0.1928%
B06.tif	1.312%	0.6636%	0.3929%	0.252%	0.1704%
B07.tif	1.079%	0.4595%	0.235%	0.04256%	0.001435%
B08.tif	1.182%	0.6272%	0.3476%	0.251%	0.1589%
B8A.tif	1.226%	0.4978%	0.2302%	0.0681%	0.0007305%
B09.tif	1.69%	0.7364%	0.4537%	0.2597%	0.1366%
B10.tif	1.88%	0.8306%	0.4938%	0.2988%	0.1995%
B11.tif	1.58%	0.8142%	0.4362%	0.267%	0.1797%
B12.tif	1.693%	0.8413%	0.4236%	0.2244%	0.1554%

**Note : These results still need to be consolidated:**

- estimating degressive trend after the 1 km measurement.
- taking care of equalization artifacts enhancing dark at values > 0 (quantization + blind pixels)

According to [RD8], straylight effects for MSI are mostly coming from optical coatings on the filters, and are characterized by large angle scattering out of the useful spectral band. However such out-of-band straylight would be characterized by an along-track offset of the straylight image (ghost). Moon observations do not provide evidence of such effect. On the contrary, straylight seems to be mostly in-band.

### 4.1.3 Synthesis and way forward

From the above analysis we can conclude that in-field straylight has a non-negligible effect (> 0.1% Lref) at least within 1 km of a bright source. This is especially true for bands B09 to B12.

The effect as observed on Moon images seems to be characterized by a homogeneous halo around the source, but no echoes (ghosts).

For RUT V1, we decide not to account for in-field straylight.

Straylight is a systematic source of error (its contribution adds a positive offset to the radiance measurement). According to GUM principles, the systematic error should first be corrected, and the residual error (linked to straylight knowledge error) should be considered as a source of uncertainty.

In the future, it could be possible to estimate this error using a convolution by an empirical kernel fitted on Moon images. However, it is not possible from Moon images to determine the spectral origin of the straylight. A practical approach could be to build a panchromatic image, estimate the total straylight from this image, and then assign it to the various spectral channels according to empirical coefficients. This estimation is not expected to be sufficiently reliable to implement a straylight correction, but it could be considered in the total uncertainty budget.

For future Sentinel missions, a more detailed characterization of the straylight impact is recommended (using monochromatic sources and analysing the dependence in the field of view).

## 4.2 Out-of-field straylight

This contribution refers to the out-of-field stray-light measured during nominal Earth observation that is not measured during calibration due to different angular configuration. This effect depends on the presence of bright objects outside of the field of views (e.g. clouds).


This effect of the Earth out-of-field stray-light is separated in 2 contributions, first a systematic one, that has been analyzed as lower than 0.3% of Lref [RD1]. Ground characterization tests were performed using a light source positioned outside of the instrument field of view, but the results were not sufficiently reliable to consider for the uncertainty analysis (Airbus France personal communication). As for in-the-field straylight, the GUM methodology requires to first correct the systematic error introduced by the straylight and then treat the residual error as a source of uncertainty. The situation for the out-of-field straylight is somewhat worse than for the in-the-field straylight as the sources of straylight for a given acquisition are not known (position and intensity), so there is no possibility to correct for its impact. Secondly, a random contribution of the out-of-field straylight is considered, results of the “undesired light” impacting the focal plan, affecting only the VNIR bands. The random contribution has been analysed by AIRBUS and the following coefficients are used. This term is summed quadratically in the uncertainty budget.

	B01	B02	B03	B04	B05	B06	B07	B08	B8A	B09	B10	B11	B12
Out-of-field straylight (random part)	0.1	0.1	0.08	0.12	0.44	0.16	0.26	0.26	0.04	0.8	0	0	0

### 4.2.1 Impact analysis

Out of Field straylight is difficult to assess since:

- ❖ Accurate ground tests are not available: Tests seemed to have been performed in the sense of compliance with the requirements, and not to accurately estimate the residuals.

	<p><b>OPT-MPC</b></p> <p><b>RUT error sources analysis</b></p>	<p>Ref.: OMPC.ACR.MEM.41</p> <p>Issue: 1.0</p> <p>Date: 01/08/2025</p> <p>Page: 13</p>
--	--	--

- ❖ The knowledge of out of field sources of straylight is not straightforward, and would need additional means of wide field observations (on the same platform or using concomitant acquisitions from other missions, ex: geostationary?)

Note that we have found no indication of a significant out-of-field straylight contribution on EO images when compared to other reference measurements.

#### 4.2.2 Model

[RD1] assumed a model with two contributors: a uniform term (constant across the field of view) equal to 0.3% of  $L_{ref}$  and a non-uniform term (with a different level for each pixel), provisionally set to 0.

The assumption of 0.3% of  $L_{ref}$  reflects the lack of knowledge of the straylight sources outside of the field of view. However, this assumption may be very conservative for ocean scenes. An alternative model assumes that the radiance level outside of the field of view is comparable to the level inside. The straylight error is modelled as 0.3% of  $L_{mean}$ , where  $L_{mean}$  is the average radiance in the image, computed for each spectral band.

#### 4.2.3 Synthesis and way forward

At the present time, there is no way to correct for out-of-field straylight or even account for its impact on uncertainty. We therefore keep the approach of [RD1] where a systematic term representing our best knowledge of the error is added to the total uncertainty, while the residual (random) error is considered in the standard uncertainty budget.

In many situations, one can assume that the out-of-field straylight is very small. In such cases, it is possible to disable the out-of-field straylight model in the RUT by configuration.

For future Sentinel missions, it could be useful to add small wide field camera (panchromatic) to identify possible sources outside of the field of view. More detailed on-ground characterization of the impact is also recommended.

### 4.3 Correlation

The straylight contribution is strongly correlated. Spatially, adjacent pixels will be affected by similar levels of straylight. Temporally, a pixel in the vicinity of a bright source will be constantly affected by a similar level of straylight. The correlation will be also high between satellite units as straylight characteristics are expected to be similar.

If a straylight correction was applied, the residual error should be much less correlated.

## 5 Electronic Cross-talk

### 5.1 Standard (linear) cross-talk

#### 5.1.1 Description and correction

A small electronic cross-talk affects the SWIR detectors of MSI. This effect introduces a small fraction of the signal of some bands into the signal of other bands. This effect is deterministic and can be compensated (cross-talk correction). The figure below illustrates the efficiency of the correction.

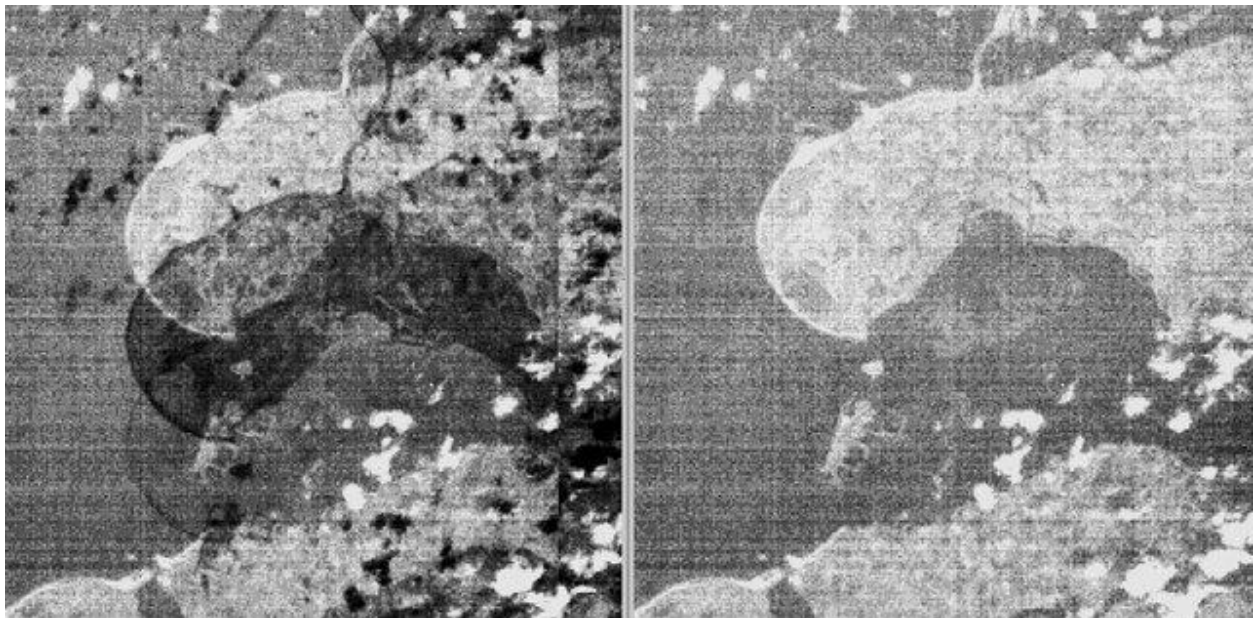



**Figure 4:** Left: L1B image of a SWIR band affected by cross-talk. Right: same image after cross-talk correction.

Tables below provide the values for S2A and S2B (rows: affected band / lines: input band).

**Table 5:** Electronic Cross-talk coefficients for Sentinel-2 models A and B.

S2A	B10	B11	B12
B10	0.00E+00	-3.98E-03	-1.78E-03
B11	-2.82E-05	0.00E+00	-2.00E-03
B12	-7.94E-04	-1.78E-04	0.00E+00

S2B	B10	B11	B12
B10	0.00E+00	-3.98E-03	-1.78E-03
B11	0.00E+00	0.00E+00	-2.00E-03
B12	-7.94E-04	-2.24E-04	0.00E+00

	<p><b>OPT-MPC</b></p> <p><b>RUT error sources analysis</b></p>	<p>Ref.: OMPC.ACR.MEM.41</p> <p>Issue: 1.0</p> <p>Date: 01/08/2025</p> <p>Page: 15</p>
--	--	--

### 5.1.2 Correction residual

The residual of this correction (due to knowledge error on the cross-talk coefficient) can be considered as an error source. It is reasonable to assume that the residual cross-talk is not larger than 1% of the nominal cross-talk. In the worst-case (B11 to B0 cross-talk) the residual would then be of the order of  $-4 \cdot 10^{-5}$  of the B11 signal. This can be considered negligible (well below one L1B DC in most cases).

## 5.2 Other cross-talk effects

---

Other more complex cross-talk effects have been observed.

### **Detector boundary effects**

Pixels located close to the edges (blind pixels) of the detectors are less affected by cross-talk [RD5]. This leads to an over-correction if the same cross-talk coefficients are applied to all pixels. However, this effect should be masked at L1C if the inter-detector area is cut at a sufficient distance from the boundaries. While this is not the case for operational products at the time of writing, improvements of the inter-detector area are planned for the near future. Therefore, we propose not to model this error source for the L1C RUT.

### **Non-linear cross-talk**

Non-linear cross-talk effects have been observed on some B10 detectors of S2D [RD4]. A possible correction has been studied but its implementation was considered relatively complex. It could be possible however to provide a worst-case estimate of this effect, which could be added to the uncertainty for the detectors concerned.

For the time being, this error source will not be modeled in the L1C RUT.

### **Gradient cross-talk**

This effect has been identified for SWIR bands during S2A commissioning and observed in S2B and S2C images. The cross-talk signal injected in the affected band is approximately proportional to the vertical gradient of the signal in the source band.

This effect can reach several LSB and can be visible in the Sea on coastal areas located close to bright landscapes (see figure below). No operational correction is envisaged for this effect.

As the effect is proportional to the gradient, the artefact is affecting the high frequencies. The average signal level is less affected, even if the artifact is visually strong.

For the time being, this error source will not be modelled in the L1C RUT.

However, some algorithms can be envisaged for a next version of the tool:

- The level of artifacts is predictable considering the gradient of the source image, a proportional factor (depending on the bands, to be evaluated) and the temporal shift between the different bands. The prediction needs to be performed in focal plane

geometry. Depending on detector oddity, the artifact is seen before or after the acquisition of the source band.

Example of Crosstalk Gradient from B11 to B12 in tile T36RYR (Warm Saoudi desert Coast). Reflectance level of the coast is around 0.5 for B11. It is generating artifacts up to 0.001 in reflectance, which is twice the reflectance of the Sea observed in the area.

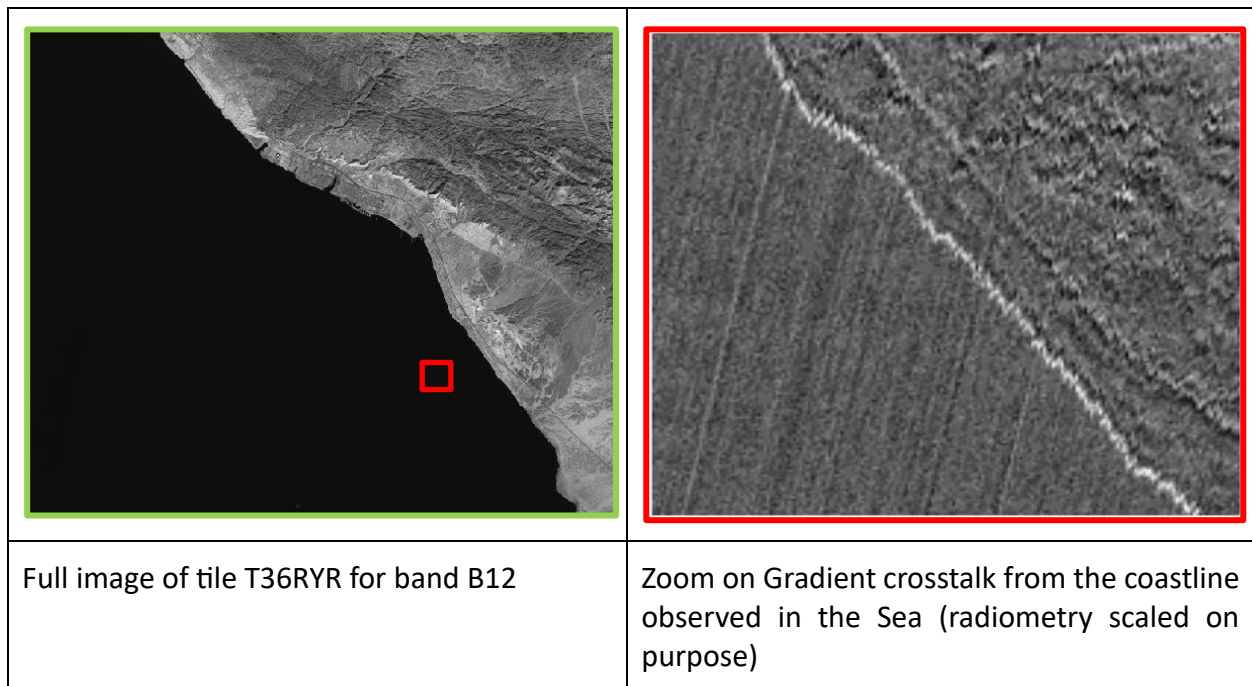


**Figure 5: Example of impact of gradient crosstalk.**

## 6 Polarization sensitivity

### 6.1 Impact analysis

Specification DG-MSI-627 requires the polarization sensitivity to remain below 5%, with a goal of 3%. Engineering budgets ([RD8], see table 5 below) reported an expected value of 2% for the VNIR and 2.65% for the SWIR.

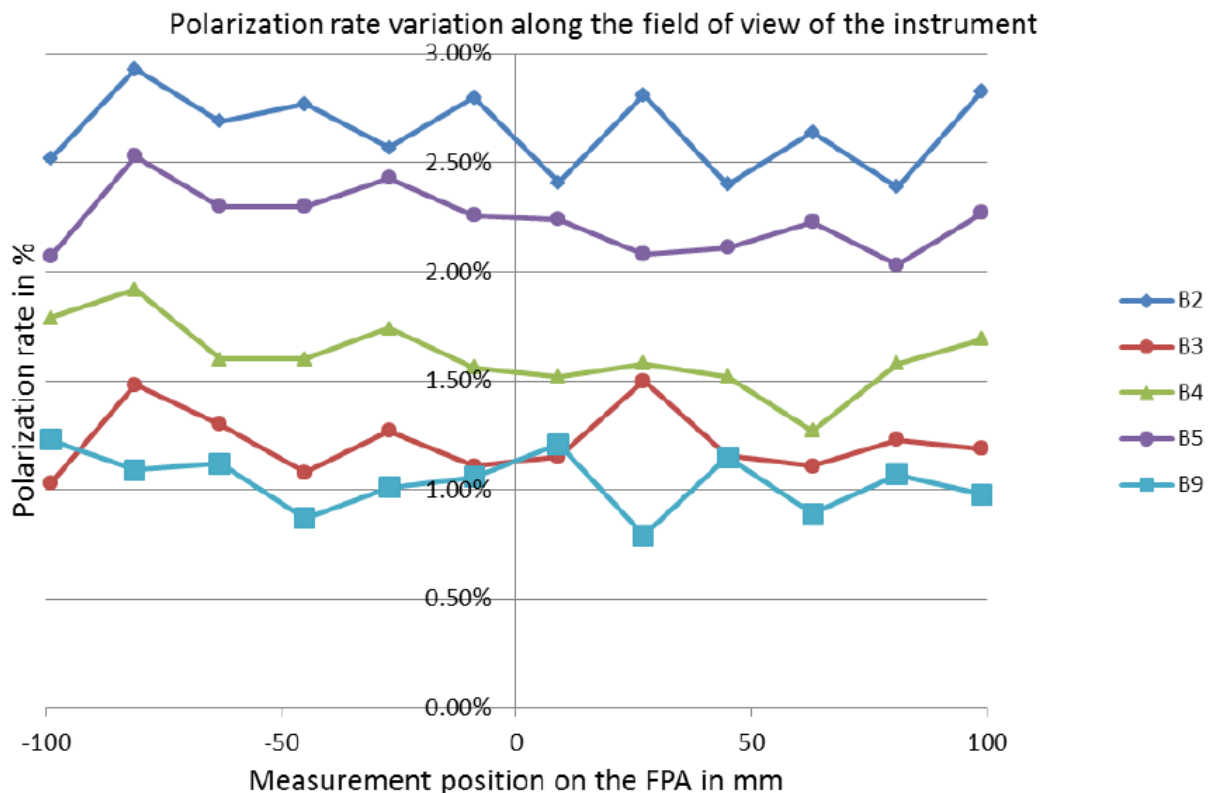
**Table 6: Polarization sensitivity budget [RD8 quoting RD-4].**

	Reference	Allocation	Expected BOL/EOL
Budget VNIR		4 %	2.0 %
Budget SWIR		4.5 %	2.65 %
Specification	DG-MSI-627	< 5 % (goal 3%)	


  

	B8	B8a	B9	B10	B11	B12
@Lmin	7.31%	8.40%	10.50%	13.90%	8.90%	33.08%
@Lref	0.41%	0.43%	0.78%	0.63%	0.65%	0.59%
% of Lref where spec is met	17%	22%	74%	55%	58%	53%

In addition, some characterization tests were performed for model A (PFM), see figure below. The performance was slightly less good than the budget, but still within the goal requirement.



**Figure 6: Measured polarization sensitivity across the field of view [RD8 quoting RD-98]**

	<p><b>OPT-MPC</b></p> <p><b>RUT error sources analysis</b></p>	<p>Ref.: OMPC.ACR.MEM.41  Issue: 1.0  Date: 01/08/2025  Page: 18</p>
--	--	--

Nevertheless, considering a scene with 10% degree of polarization, the resulting relative error could be up to 0.3%, which is not negligible. This error is systematic in the sense that repeated measurements of the same scene would lead to the same error.

## 6.2 Synthesis and way forward

---


In RUT V1, uncertainty coming from polarization is not taken into account.

For the future, we first recommend assessing more precisely the possible impact. The problem is to identify acquisitions for which polarization sensitivity could contribute significantly to the total uncertainty and more generally to quantify the likely impact. To achieve this, a possible approach could be to use Radiative Transfer (RT) simulations for typical situations (different surfaces, viewing conditions and aerosol and water vapour load).

## 6.3 Correlations

---

The degree of polarization is expected to be similar over scenes with the same surface and atmospheric conditions, which would lead to spatial correlation of the effects. There may also be a temporal correlation in some cases. The effects are also expected to be correlated across spectral bands and between satellite units.

	<p><b>OPT-MPC</b></p> <p><b>RUT error sources analysis</b></p>	<p>Ref.: OMPC.ACR.MEM.41</p> <p>Issue: 1.0</p> <p>Date: 01/08/2025</p> <p>Page: 19</p>
--	--	--

## 7 On-board compression noise

### 7.1 Description

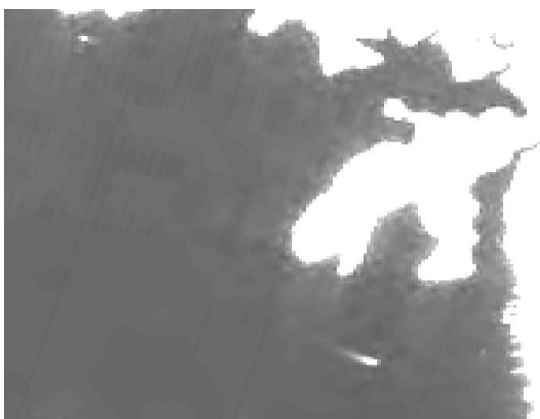
The on-board compression features of the Sentinel-2 imagery system are designed to optimize data storage ensuring image quality under the constraint of a fixed rate compression. The system employs a Multi-Resolution Compressor, which operates by bit plane and uses generic rolling buffers of 16 lines on the full detector swath (reminder, the instrument swath contains 12 detectors). The compression process involves three levels of wavelet transformation, with coding of the wavelet images by descending bit planes. The compressed data is then appended to the bit stream at the level of one block of 16 lines and one detector swath until the buffer is filled. Decompression reverses this process, reconstructing the original data by filling in any missing bits with zeros.

This approach ensures that high radiance and highly textured landscapes are compressed effectively, although it can introduce certain artifacts visible in uniform areas, such as flattening, wavelet butterflies, (and sometimes across-track and along-track lines strips). These artifacts are most visible in areas where the landscape is complex: most parts of detector swath covered by high frequencies, high radiances.

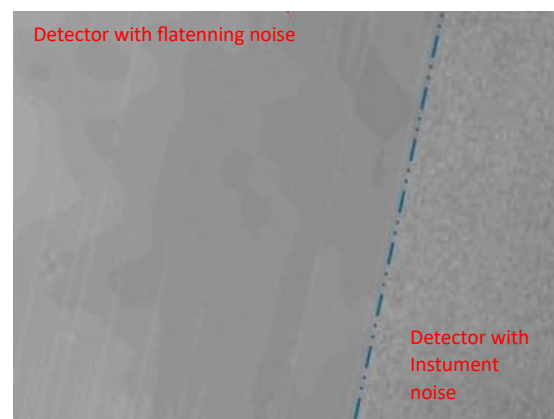
### 7.2 Impact analysis

#### 7.2.1 Flattening


Flattening occurs when the compression algorithm stops encoding at higher bit-planes in complex scenes, discarding lower bit-plane high frequencies. This results in a visually flattened effect, especially in uniform regions where subtle variations are lost.



T19TBF (01/09/2023) – New York Coast

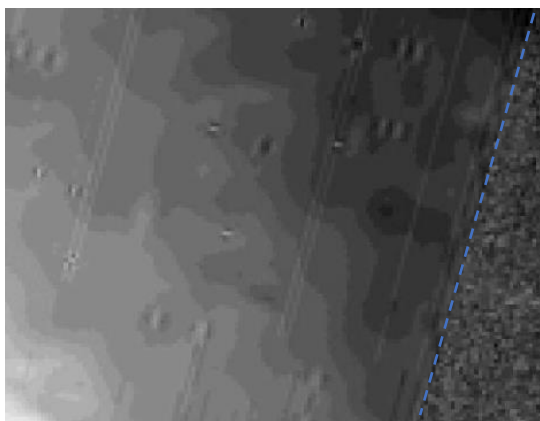


Tile T16TDN (28/08/2023) – Lake Michigan

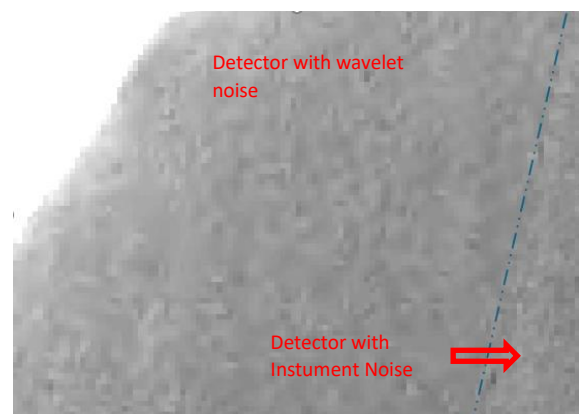
	<p><b>OPT-MPC</b></p> <p><b>RUT error sources analysis</b></p>	<p>Ref.: OMPC.ACR.MEM.41</p> <p>Issue: 1.0</p> <p>Date: 01/08/2025</p> <p>Page: 20</p>
--	--	--

## 7.2.2 Butterflies

Wavelet butterflies are structured noise artifacts caused by incomplete encoding of high-frequency wavelet coefficients. These appear as butterfly-shaped patterns, especially noticeable in flattened areas, but this kind of structured noise is present everywhere in the detector swath.



*Tile T19TCG (01/09/2023) – New York Coast*



*Tile T30TYK (23/08/2023) – Catalunya Coast*

## 7.2.3 Order of magnitude

The wavelet butterflies may be of high level (+8 LSB in worst cases). However, they are very HF localized artifacts, which are not affecting the average signal of the area.

Also, the flattening is destroying the structure of the HF noise, but the average of signal remains unchanged (in the scale of 1 LSB).

We notice here that, in the coding of one bit-plane, the algorithm begins with the LF block, and by construction of the blocks, there is a bit-plane shift between LF and HF (roughly, coding 1 LSB of LF is done 3 bit-planes higher than coding 1 LSB in HF).

This means that the low frequency of the signal (8\*8 pixels averaging) can be considered never affected (within 1 LSB margin) by the compression, considering the bit rates used in S2 compression.


## 7.3 Possible modelling approaches

### 7.3.1 Detection of flattening in the signal of blind pixels

Some studies have been performed on the blind pixels noise. The idea was to correlate the blind pixels flattening with the complexity of the swath, and the emergence of artifacts inside the useful area of the swath. Blind pixels flattening should be estimated by the reduction of Noise measured in the blind pixels compared to the foreseen instrument dark noise.

Unfortunately, besides flattening, blind pixels are also subject to wavelet butterflies which enhance the global noise measured on blind pixels.

In conclusion, no straightforward solution can be envisaged using blind pixels.

	<p><b>OPT-MPC</b></p> <p><b>RUT error sources analysis</b></p>	<p>Ref.: OMPC.ACR.MEM.41  Issue: 1.0  Date: 01/08/2025  Page: 21</p>
--	--	--

### 7.3.2 Monitoring of truncation level during decompression

A second solution is to instrument the decompression software to check/log, at each block of line, on which bit plane the coding stops. This needs to be done for each of the wavelet blocks

With this log information, it is possible to estimate the average degradation of signal (in HF, MF, LF) to be considered for the block of 16 lines in focal plane geometry.

Note that such uncertainty estimation needs to be performed in L1B geometry, in LSB, and transferred to L1C, geometrically (orthorectification) and radiometrically (from LSB to reflectance).

## 7.4 Synthesis and way forward

---

In the current version of the RUT, this effect is not modelled.

Although the error can reach non-negligible levels, it affects a very limited number of pixels. The impact at image level can therefore be considered negligible.

## 7.5 Correlation

---

Compression noise is expected to be essentially random (uncorrelated).

## 8 Spectral response knowledge

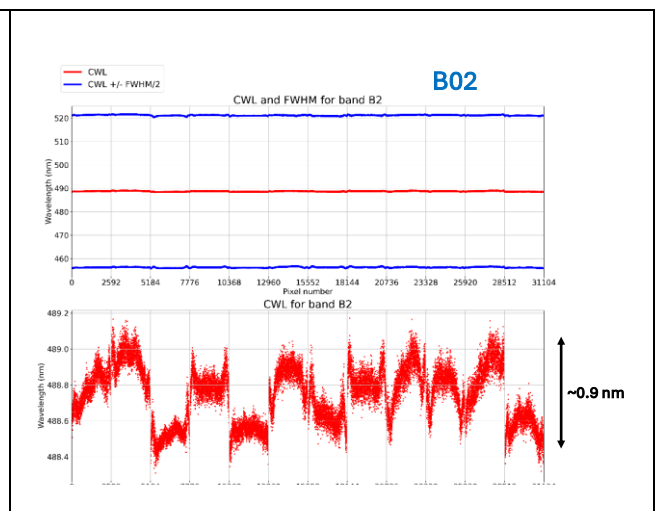
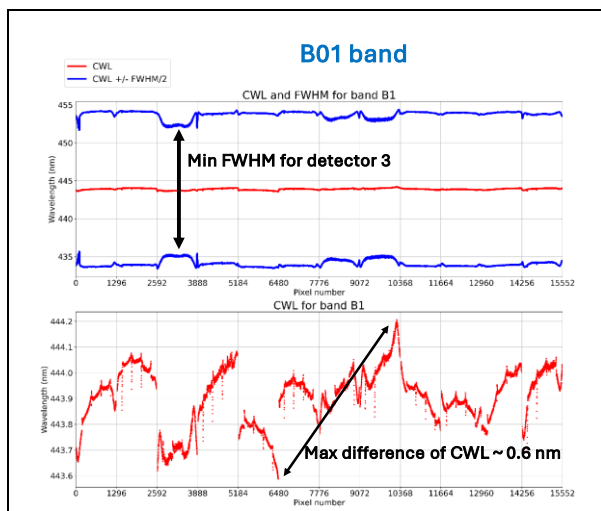
### 8.1 Description

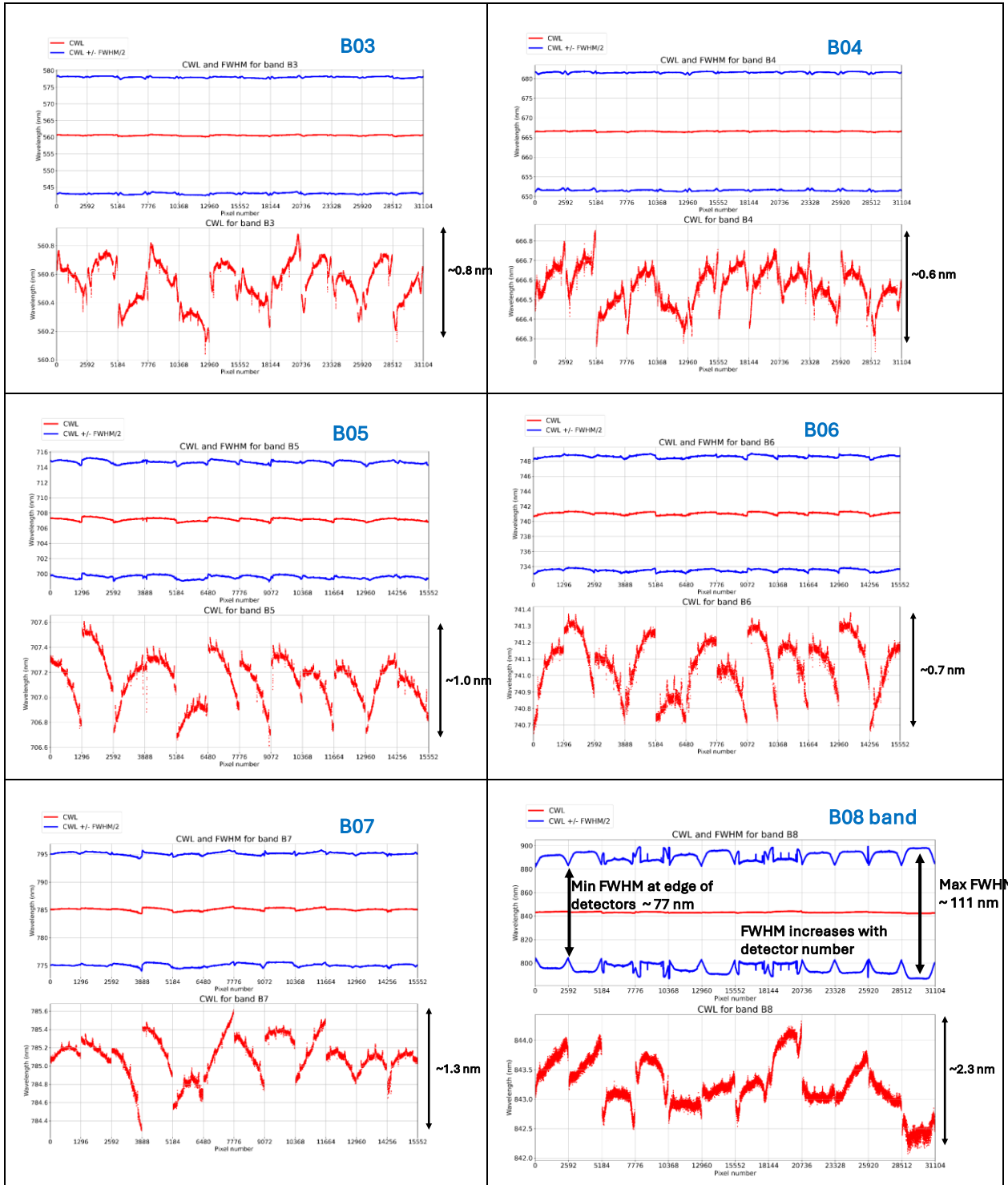
The instrument Spectral Response Function (ISRF) varies slightly from pixel to pixel. This is mainly due to inhomogeneities of the filter. These differences impact the measured TOA radiometry, which adds an error source.

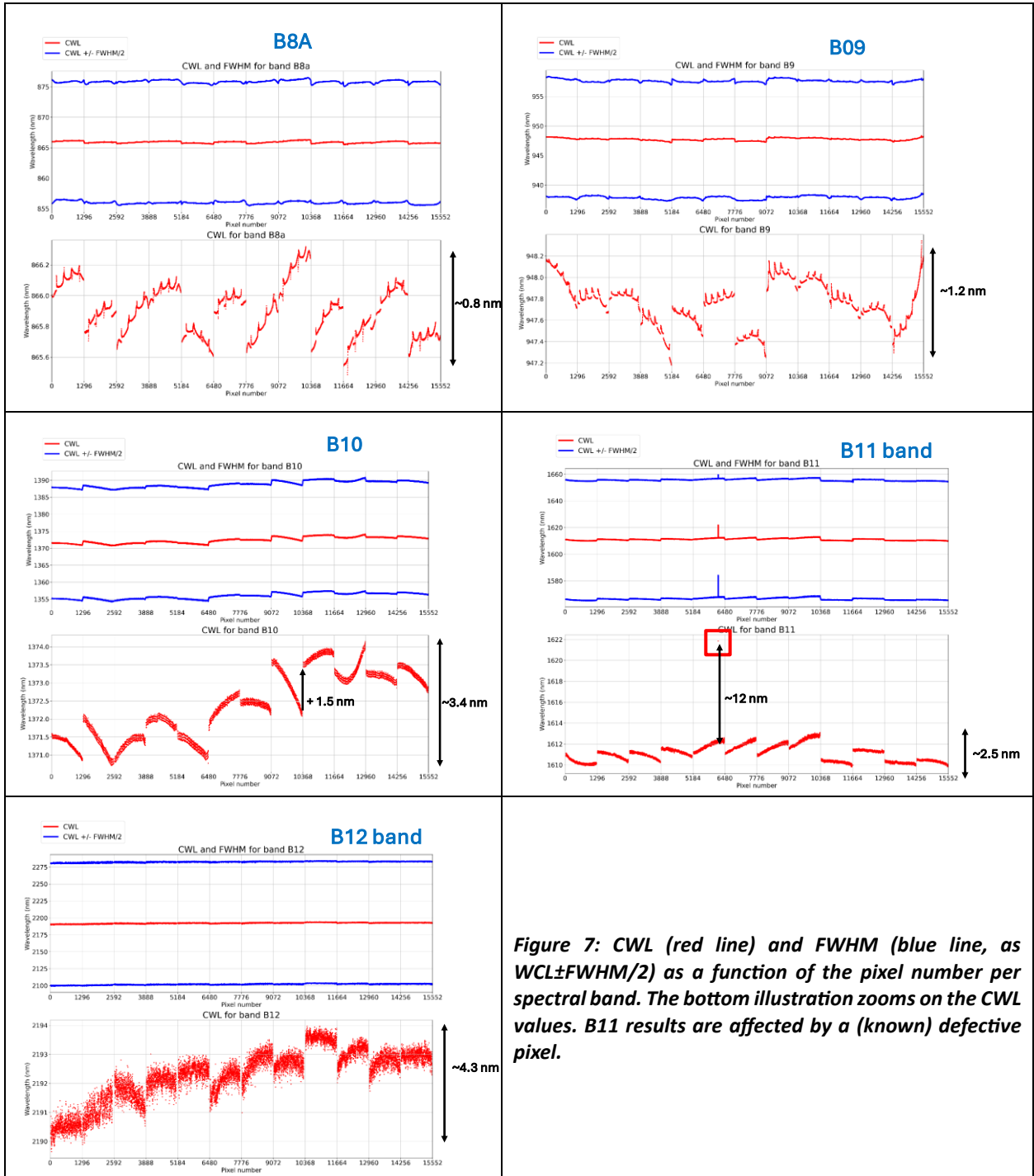
For Sentinel-2C, a detailed characterization of the spectral responses at pixel level has been performed. The results are summarized in the following table and figures.

**Table 7: Statistics on central wavelength (CWL) and full-width half-maximum (FWHM) values for S2C. Minimum, average and maximum values over all the pixels, range and standard deviation, per band. The results for B11 are affected by a (known) defective pixel.**

	CWL (nm)					FWHM (nm)				
	min	avg	max	max-min	std	min	avg	max	max-min	std
B01	443,6	443,9	444,2	0,6	0,11	16,0	19,7	20,6	4,6	0,91
B02	488,3	488,7	489,2	0,9	0,15	63,8	65,0	65,5	1,8	0,26
B03	560,0	560,5	560,9	0,8	0,15	33,8	35,0	35,5	1,7	0,31
B04	666,2	666,6	666,9	0,6	0,10	28,9	30,0	30,5	1,6	0,27
B05	706,6	707,1	707,6	1,0	0,18	14,7	15,1	15,5	0,8	0,22
B06	740,6	741,1	741,4	0,7	0,16	14,9	15,1	15,5	0,6	0,14
B07	784,3	785,1	785,6	1,3	0,21	19,5	20,0	20,6	1,1	0,32
B08	842,1	843,2	844,3	2,3	0,41	77,5	96,3	111,6	34,1	7,93
B8A	865,5	865,9	866,3	0,8	0,16	19,0	19,9	20,5	1,5	0,31
B09	947,2	947,8	948,3	1,2	0,20	19,2	19,8	20,5	1,3	0,31
B10	1370,7	1372,4	1374,1	3,4	0,91	32,7	32,9	33,4	0,7	0,14
B11	1609,8	1611,1	1621,9	12,1	0,76	75,5	89,3	89,9	14,4	0,21
B12	2189,6	2192,3	2194,0	4,3	0,88	179,0	180,8	183,1	4,1	0,50







The variations of the SRF will create small differences in the radiometry of each pixel, which will appear in the images as an additional Fixe Pattern Noise (along-track strips). The relative error depends on the scene (spectral profile) but not on the radiance level.

## 8.2 Impact analysis

To quantify the impact of the SRF differences, an approach based on radiative transfer simulations has been followed, see [RD12]. 8 different spectra have been considered:

- Seawater from the USGS spectral Library.
- Vegetation: lawn grass and cheatgrass from the USGS spectral Library.
- Few kinds of sand: one sample from the USGS spectral Library, and two samples corresponding to PICS sites (Namibia and Algeria4) from PICSAND data.
- Snow: one sample from the SISpec Snow & Ice Spectral Library.
- Urban material: concrete from the USGS spectral Library.

A reference atmosphere with a medium aerosol optical depth (0.2) and water vapour load (3 g/cm<sup>2</sup>) has been used. For each profile, a TOA radiance spectrum has been computed using a radiative transfer code. To assess the impact on L1C products, one must also take into account the impact of the SRF differences on Sun diffuser images. Indeed, these differences are corrected during the calibration process. For the latter case, a white Sun diffuser (flat spectrum) has been assumed for all bands.

Finally, [RD12] determined the range of variations (max-min) of the measured radiances after application of equalization gains. The results are summarized in the table below, and compared to the expected instrument noise for this scene. Cases for which the SRF difference impact is higher than the measurement noise are highlighted with an orange background.

**Table 8: Dispersion of TOA radiance per band, for each type of surface (after application of equalization coefficients).**


Band	Surface	TOA CORRECTED EQUAL RADIANCE					Noise@L
		Ltoa			$\Delta L$	$\Delta L / L_{avg}$	
		min	moy	max			
B1	Cheatgrass	65.90	65.97	66.03	0.13	0.2%	0.15
B1	Lawn Grass	60.23	60.31	60.39	0.17	0.3%	0.15
B1	Sand	78.94	78.98	79.03	0.09	0.1%	0.16
B1	Seawater	63.87	63.99	64.12	0.24	0.4%	0.15
B1	Concrete	121.86	121.89	121.90	0.03	0.0%	0.19
B1	Snow	372.28	372.43	372.48	0.20	0.1%	0.29
B1	Namibie	90.46	90.50	90.58	0.13	0.1%	0.17
B1	Algerie4	93.47	93.52	93.57	0.10	0.1%	0.17
B2	Cheatgrass	59.93	59.99	60.06	0.13	0.2%	0.40
B2	Lawn Grass	51.35	51.44	51.50	0.16	0.3%	0.37
B2	Sand	76.14	76.18	76.22	0.08	0.1%	0.45
B2	Seawater	50.02	50.17	50.32	0.30	0.6%	0.37
B2	Concrete	125.47	125.50	125.52	0.05	0.0%	0.57
B2	Snow	380.30	380.36	380.42	0.12	0.0%	0.98
B2	Namibie	89.74	89.80	89.84	0.09	0.1%	0.48

B2	Algerie4	96.39	96.45	96.48	0.10	0.1%	0.50
B3	Cheatgrass	49.26	49.28	49.31	0.05	0.1%	0.34
B3	Lawn Grass	49.49	49.62	49.79	0.30	0.6%	0.34
B3	Sand	69.28	69.29	69.30	0.02	0.0%	0.40
B3	Seawater	27.95	28.01	28.10	0.15	0.5%	0.26
B3	Concrete	118.20	118.21	118.25	0.05	0.0%	0.52
B3	Snow	328.81	329.01	329.27	0.46	0.1%	0.86
B3	Namibie	92.60	92.74	92.84	0.24	0.3%	0.46
B3	Algerie4	113.17	113.54	113.81	0.65	0.6%	0.51
B4	Cheatgrass	56.92	57.04	57.16	0.24	0.4%	0.32
B4	Lawn Grass	22.24	22.25	22.27	0.03	0.1%	0.21
B4	Sand	64.30	64.37	64.44	0.15	0.2%	0.34
B4	Seawater	16.17	16.17	16.18	0.01	0.1%	0.18
B4	Concrete	107.59	107.69	107.82	0.24	0.2%	0.44
B4	Snow	282.09	282.36	282.71	0.62	0.2%	0.71
B4	Namibie	109.68	109.83	110.00	0.32	0.3%	0.45
B4	Algerie4	159.76	160.01	160.27	0.52	0.3%	0.54
B5	Cheatgrass	62.48	62.73	62.94	0.47	0.7%	0.26
B5	Lawn Grass	46.25	47.40	48.39	2.14	4.5%	0.23
B5	Sand	60.22	60.33	60.44	0.22	0.4%	0.25
B5	Seawater	13.31	13.32	13.33	0.02	0.2%	0.14
B5	Concrete	96.71	96.83	96.96	0.25	0.3%	0.31
B5	Snow	248.28	248.54	248.84	0.56	0.2%	0.49
B5	Namibie	103.71	103.91	104.10	0.39	0.4%	0.32
B5	Algerie4	152.36	152.67	152.95	0.59	0.4%	0.39
B6	Cheatgrass	68.18	68.62	68.93	0.76	1.1%	0.26
B6	Lawn Grass	141.71	143.72	145.16	3.44	2.4%	0.38
B6	Sand	59.42	59.76	59.98	0.56	0.9%	0.25
B6	Seawater	11.45	11.48	11.50	0.05	0.5%	0.12
B6	Concrete	90.69	91.16	91.48	0.80	0.9%	0.30
B6	Snow	229.06	230.29	231.09	2.03	0.9%	0.47
B6	Namibie	101.17	101.75	102.14	0.97	1.0%	0.32
B6	Algerie4	149.84	150.72	151.31	1.47	1.0%	0.39
B7	Cheatgrass	72.49	72.52	72.53	0.04	0.1%	0.26
B7	Lawn Grass	180.25	180.42	180.66	0.41	0.2%	0.40
B7	Sand	57.59	57.65	57.72	0.13	0.2%	0.24
B7	Seawater	9.63	9.65	9.68	0.05	0.5%	0.12
B7	Concrete	83.86	83.98	84.17	0.31	0.4%	0.28
B7	Snow	202.60	203.01	203.65	1.05	0.5%	0.43
B7	Namibie	96.75	96.87	97.04	0.29	0.3%	0.30
B7	Algerie4	144.01	144.19	144.45	0.44	0.3%	0.36
B8	Cheatgrass	67.25	67.80	68.25	1.00	1.5%	0.35
B8	Lawn Grass	149.98	150.83	151.26	1.28	0.8%	0.52
B8	Sand	48.69	48.92	49.03	0.34	0.7%	0.30
B8	Seawater	7.45	7.54	7.62	0.17	2.2%	0.13
B8	Concrete	67.83	68.41	68.80	0.96	1.4%	0.35
B8	Snow	160.59	161.75	162.88	2.29	1.4%	0.54
B8	Namibie	78.64	79.20	79.56	0.93	1.2%	0.38

B8	Algerie4	118.82	119.66	120.13	1.31	1.1%	0.46
B8A	Cheatgrass	75.98	76.05	76.11	0.14	0.2%	0.35
B8A	Lawn Grass	157.63	157.67	157.72	0.09	0.1%	0.49
B8A	Sand	51.40	51.42	51.44	0.04	0.1%	0.29
B8A	Seawater	7.23	7.23	7.24	0.00	0.1%	0.12
B8A	Concrete	70.31	70.33	70.35	0.04	0.1%	0.33
B8A	Snow	164.03	164.14	164.27	0.24	0.1%	0.50
B8A	Namibie	81.21	81.22	81.25	0.03	0.0%	0.36
B8A	Algerie4	124.58	124.63	124.69	0.11	0.1%	0.44
B9	Cheatgrass	11.62	11.94	12.25	0.62	5.2%	0.08
B9	Lawn Grass	20.21	20.75	21.27	1.07	5.1%	0.10
B9	Sand	7.54	7.74	7.93	0.39	5.0%	0.07
B9	Seawater	1.63	1.65	1.68	0.04	2.6%	0.05
B9	Concrete	9.73	9.99	10.24	0.51	5.1%	0.07
B9	Snow	19.82	20.36	20.88	1.06	5.2%	0.09
B9	Namibie	10.96	11.27	11.56	0.59	5.3%	0.08
B9	Algerie4	17.28	17.77	18.24	0.96	5.4%	0.09
B10	Cheatgrass	0.08	0.08	0.08	0.00	3.3%	0.02
B10	Lawn Grass	0.08	0.08	0.08	0.00	3.8%	0.02
B10	Sand	0.08	0.08	0.08	0.00	2.7%	0.02
B10	Seawater	0.08	0.08	0.08	0.00	1.1%	0.02
B10	Concrete	0.08	0.08	0.08	0.00	2.8%	0.02
B10	Snow	0.08	0.08	0.08	0.00	2.6%	0.02
B10	Namibie	0.08	0.08	0.08	0.00	3.6%	0.02
B10	Algerie4	0.08	0.08	0.08	0.00	4.7%	0.02
B11	Cheatgrass	18.41	18.42	18.46	0.05	0.3%	0.04
B11	Lawn Grass	17.44	17.50	17.60	0.15	0.9%	0.04
B11	Sand	16.21	16.23	16.25	0.04	0.3%	0.03
B11	Seawater	1.20	1.20	1.20	0.00	0.1%	0.02
B11	Concrete	18.73	18.74	18.76	0.03	0.1%	0.04
B11	Snow	2.41	2.43	2.45	0.04	1.8%	0.02
B11	Namibie	26.58	26.59	26.61	0.02	0.1%	0.04
B11	Algerie4	37.56	37.57	37.60	0.04	0.1%	0.05
B12	Cheatgrass	4.11	4.12	4.12	0.01	0.3%	0.01
B12	Lawn Grass	2.79	2.80	2.81	0.02	0.6%	0.01
B12	Sand	4.90	4.91	4.91	0.01	0.2%	0.01
B12	Seawater	0.32	0.32	0.32	0.00	0.2%	0.01
B12	Concrete	6.17	6.18	6.18	0.01	0.2%	0.01
B12	Snow	0.68	0.69	0.69	0.01	2.1%	0.01
B12	Namibie	7.71	7.72	7.73	0.02	0.2%	0.01
B12	Algerie4	11.57	11.58	11.60	0.02	0.2%	0.02

The analysis shows that:

- The SRF differences have an impact higher than 0.1% for most cases and generally above the noise level for bands B05, B06, B07, B08, B11 and B12.

	<p><b>OPT-MPC</b></p> <p><b>RUT error sources analysis</b></p>	<p>Ref.: OMPC.ACR.MEM.41  Issue: 1.0  Date: 01/08/2025  Page: 28</p>
--	--	--

- For B09 and B10 the impact is also significant, but since they are purely atmospheric bands, the impact on downstream products will be limited.
- As expected, the impact depends strongly on the type of surface.

### 8.3 Way forward

---

At this stage, there does not seem to be an easy way to model this error source. Indeed, the impact depends strongly on the spectral profile of the observed scene, an information which is not available. A possibility could be to use a coarse scene classification to identify areas where the impact is expected to be more significant. This solution is not easy to implement and may not provide very effective predictions.


In the RUT V1, this term is not implemented.

### 8.4 Correlation

---

The error depends on the pixel and the spectral content of the scene. Therefore, the error will be correlated spatially (in the along-track direction) and temporally as long as long the spectrum remains the same. There is also a partial correlation in the across-track direction for some bands.

There is however no inter-band correlation.

	<p><b>OPT-MPC</b></p> <p><b>RUT error sources analysis</b></p>	<p>Ref.: OMPC.ACR.MEM.41  Issue: 1.0  Date: 01/08/2025  Page: 29</p>
--	--	--

## 9 Radiometric calibration uncertainty

### 9.1 Description

---

#### 9.1.1 Gains

The radiometric gains (absolute gain and relative equalization gain) are determined from Sun diffuser acquisitions. They are affected by several effects:

- Diffuser reflectance knowledge (mean value and angular effects)
- Diffuser reflectance temporal drift (ageing)
- Straylight in calibration mode
- Diffuser polarization
- Sun/Diffuser angular knowledge error (cosine effect)

The gains (in radiance units) also depend on the estimation of the solar band irradiance. However this term cancels out when converting to reflectance at L1C and cannot therefore be ignored.

Errors in absolute gains can be assessed by vicarious methods. Errors in relative gains can be separated in low frequency and high frequency components. High frequency components are known as Pixel Response Non Uniformity (PRNU), a contributor to the Fixed Pattern Noise (FPN). The FPN is monitored on L1B images and shown to be lower than 0.1% (at radiances close to  $L_{ref}$ ) for most pixels and therefore negligible. The contribution is generally higher for SWIR bands, the cirrus band B10 being the worst case. The error is essentially due to the temporal stability of the pixel response and increases slowly with time since the last calibration.

#### 9.1.2 Offsets

The calibration of the L1A signal also involves an offset correction (dark signal subtraction). The dark signal for each pixel is computed by averaging dark calibration images.

Residual errors on the dark signal result in Dark Signal Non-Uniformity (DSNU), the other contributor to the FPN. The DSNU has more significant impact at low radiances (see figure below). This contribution is also considered negligible with respect to the dark noise.

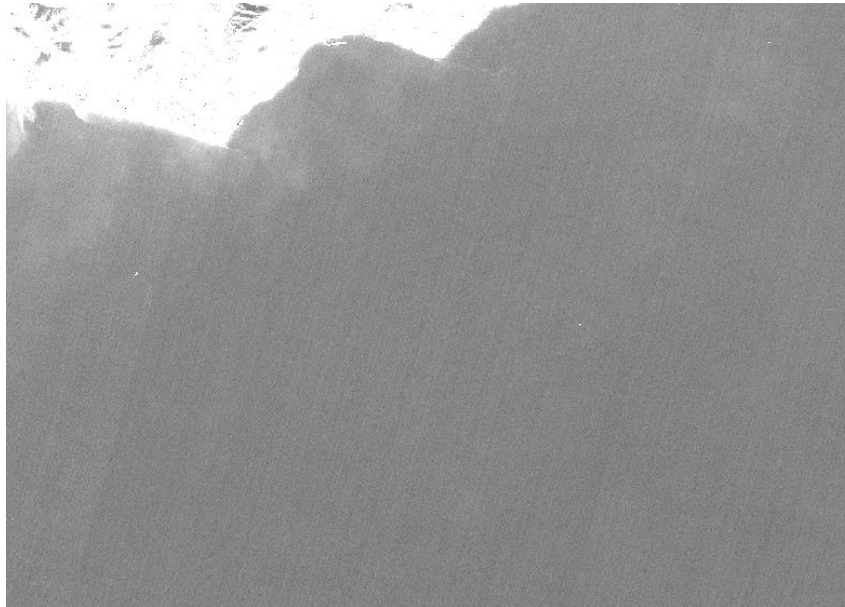


**Figure 8: Coastal scene showing Fixed Pattern Noise effects (tile 32TLP, 07/12/2021, band B04).**

A further correction is applied to each detector line using the blind pixels. This correction compensates potential thermal effects. This correction being very small, residuals are considered negligible.

The random dark noise is handled separately by the noise model.

## 9.2 Modelling

The Diffuser reflectance absolute knowledge has been carefully assessed pre-flight and reported into the ICCDB []. The figures regarding the associated uncertainty describe the diffuser reflectance absolute uncertainty due to the calibration, but also other secondary effects related to the angular, spatial and polarisation performance, as mentioned in [RD1].

**Table 9: Diffuser Reflectance absolute knowledge error in percentage, extracted from ICCDB**

Sensor	B01	B02	B03	B04	B05	B06	B07	B08	B8A	B09	B10	B11	B12
Sentinel-2A	1.09	1.08	0.84	0.73	0.68	0.97	0.83	0.81	0.88	0.97	1.39	1.39	1.58
Sentinel-2B	1.16	1.00	0.79	0.70	0.85	0.77	0.80	0.8	0.85	0.66	1.70	1.46	2.13
Sentinel-2C	0.86	0.79	0.79	0.63	0.74	0.73	0.69	0.59	0.66	0.61	1.59	1.44	1.89

The angular knowledge effect (cosine effect) has been well characterised pre-flight. The vibration tests and the previously mentioned thermal cycling test reported a diffuser planarity of 0.13. This uncertainty source is propagated with an estimated effect of 0.4% ( $k = 1$ ).

The straylight in calibration mode is caused by the specific orientation of the instrument and the shutter mechanism, meaning the sunlight enters the instrument through multiple reflections. This same situation does not occur during the imaging of the Earth and introduces a systematic error

in the calibration coefficient. The pre-flight analysis evaluated this error as 0.7% of the diffuser radiance. A correcting factor has been introduced, so it is the knowledge on this correction that needs to be accounted for in the uncertainty budget. A residual of 0.3% has been allocated for this contributor. This is a conservative evaluation that is expected to be revisited if possible. While the diffuser absolute knowledge could be seen as a systematic effect, the knowledge of the effect is representative of the dispersion around the measured value. The 3 previous contributions will therefore be summed quadratically.

$$u_{diffuser} = \sqrt{u_{reflectance\ knowledge}^2 + u_{cosine}^2 + u_{calibration\ straylight}^2}$$

The diffuser reflectance temporal drift (ageing) represents a systematic effect that evolve with time. It is not possible to correct for it, this will “enlarge” the expanded uncertainty estimate by adding this component linearly. A contribution is foreseen in the tool and can be configured. But calibration measurements over 10 years show that the ageing of the S2 diffuser is very limited which is consistent with the pre-flight test made simulated ageing of the diffuser. For RUTv1 we recommend deactivating this contribution.

### 9.3 Synthesis and way forward

In RUT V1, three of the four diffuser uncertainty contributors considered, are estimated based on pre-launched calibration. Their knowledge appears aligned with the known performances of the instrument. The fourth term, the diffuser temporal drift, has been showed negligible and is therefore disabled.

If a temporal drift should become measurable in the future, it will be necessary to account for it in the RUT, by possibly derived a temporal model computing the resulting bias as a function of the acquisition time.


### 9.4 Correlation

The following table provides an assessment of the correlations of the different error sources.

**Table 10: Existing correlations for the difference calibration error sources.**

Error source	Status	Correlations
Diffuser absolute reflectance knowledge error	modelled	Systematic uncertainty, spatially and temporally correlated Probably spectrally correlated
Diffuser angular response knowledge error	modelled	Seasonal calibration errors Radiometric spatial non-uniformity error

Dark signal knowledge error in calibration mode	negligible	Contribution to FPN: temporal correlation (along columns)
Additional straylight in calibration mode	modelled	Systematic uncertainty, spatially and temporally correlated Spectrally correlated
Sun-Diffuser angular knowledge error	modelled	Systematic uncertainty, spatially and temporally correlated Spectrally correlated
Sensor response temporal stability	negligible	Contribution to FPN: temporal correction (along columns)

	<p><b>OPT-MPC</b></p> <p><b>RUT error sources analysis</b></p>	<p>Ref.: OMPC.ACR.MEM.41</p> <p>Issue: 1.0</p> <p>Date: 01/08/2025</p> <p>Page: 33</p>
--	--	--

## 10 Orthorectification: noise filtering

### 10.1 Description

---

The L1C processing involves the orthorectification to generate images in UTM projection. This is done using a cubic spline resampling. It is therefore necessary to propagate the L1B uncertainty through this process.

Errors with are constant spatially are not impacted by the resampling. In the current RUT implementation, the instrument noise is the only term that needs to be propagated, but in principle other terms should also be propagated (e.g. non-linearity residual).

With a cubic spline interpolation, the L1C value on each pixel depends in a non-linear way on input L1B values of all pixels. However, the sensitivity decreases with the distance to the interpolated point. If the interpolation point falls very close to a point from the L1B grid, the point value will be close to the original value and the noise reduction will be small. If on the other hand the interpolation point falls near a corner of the L1B pixel, the value will be a combination of the values from several pixels and the noise will be reduced. Following the principles described in the introduction, it is sufficient to model the average impact. Note in some cases, due to the non-linear nature of the cubic spline interpolation, the noise could also be amplified.

### 10.2 Modelling

---

We follow the empirical approach proposed by [RD10]. The method relies on the determination of noise levels on L1B patches and corresponding L1C patches. The ratio between the SNR at L1B and L1C was shown to be in the range 0.5 to 0.75, with a mean value close to 0.65.

The proposed model therefore computes the expected noise level using the L1B noise model and applies a coefficient of 0.65 to compute the L1C noise.


This method is implemented in the current version of the S2RUT. The smoothing parameter can be adjusted by a configuration file.

### 10.3 Way forward

---

The current approach gives a reasonable account of the noise reduction after resampling. However it is not suitable to propagate other error terms. A fully rigorous approach to propagate the L1B uncertainty would require computing the sensitivity of the L1C value to each input L1B value, taking into account the correlation of the errors between the different L1B pixels. This would require an implementation within the L1B processor and would be an extremely complex task.

While this approach does not seem practical even as a long-term goal, it could be nevertheless interesting to study a few test cases to get a better insight into the actual impact of resampling (see also next section). For this, a set of Monte Carlo samples could be generated by adding noise to a reference (“noiseless”) image. The image could be resampled on a grid shifted by a fixed

 <p><b>OPT-MPC</b> Copernicus Sentinel Optical Mission Performance Cluster</p>	<p><b>OPT-MPC</b></p> <p><b>RUT error sources analysis</b></p>	<p>Ref.: OMPC.ACR.MEM.41 Issue: 1.0 Date: 01/08/2025 Page: 34</p>
--	--	---

distance in column and rows and the noise computed on the resample image using the Monte Carlo samples.

## 10.4 Correlation

---

After propagation to L1C, the sensor noise becomes locally spatially correlated.

## 11 Orthorectification: resampling error

### 11.1 Description

This section describes a different effect of the orthorectification step, which would occur even in absence of any L1B uncertainty (“perfect image”). The interpolation error depends on the other hand on the texture of the image: in case of a uniform or very smooth image, the interpolation would not add any error. According to the theory (Hall and Meyer, 1976), the interpolation error for cubic-spline interpolation a smooth function depends on the fourth derivative of the function. However Earth Observation images are generally not smooth so this theorem is not directly applicable. The impact of the resampling error will depend on the actual spectral profile of EO images for a given sensor Point-Spread Function (PSF).

### 11.2 Modelling

To investigate and model the interpolation error, several authors propose an empirical approach ([RD-10], [RD-11]).


[RD-10] uses high-resolution aerial images to generate pseudo L1C images and assess the interpolation error. The author builds an empirical model linking the interpolation error computed at the corners of the pixels (worst-case) to the standard deviation of a (2 x 2)-pixel L1C image patches.

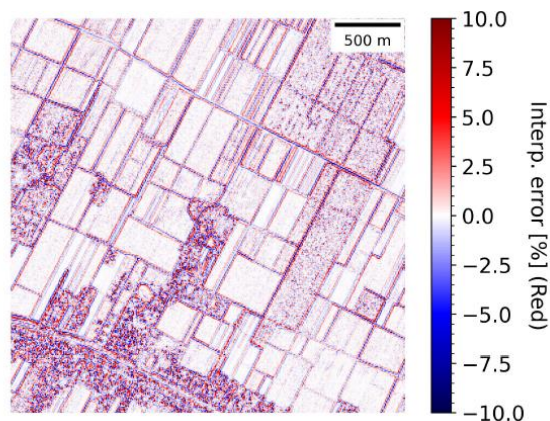


**Figure 9: Interpolation error from image simulation, from [RD-10].**

[RD11] uses simulated images with Gaussian and Sigmoid profiles to analyse the interpolation error. A look-up-table is generated to compute the local error based on the Discrete Fourier Transform coefficients computed on 4-pixel patches and the interpolation offset to the initial grid points. This method uses L1R images (equivalent of L1B in Landsat context) in input.

In the current version of the RUT, the resampling error is not modelled.

	<p><b>OPT-MPC</b></p> <p><b>RUT error sources analysis</b></p>	<p>Ref.: OMPC.ACR.MEM.41  Issue: 1.0  Date: 01/08/2025  Page: 36</p>
--	--	--

### 11.3 Way forward


---

In the future, the image simulation approach of [RD10] could be reproduced, and alternative modelling approaches investigated (e.g. machine learning). The approach of [RD10] assumes a worst-case situation (interpolation at the corners of the pixels) in order to work from L1C images. An implementation in the L1B processor (as in [RD11]) could consider the actual value of the offset.

### 11.4 Correlation

---

The interpolation error is spatially locally correlated. In addition, as it depends on the frequency content of the scene, the errors will be partially correlated over time.

	<p><b>OPT-MPC</b></p> <p><b>RUT error sources analysis</b></p>	<p>Ref.: OMPC.ACR.MEM.41  Issue: 1.0  Date: 01/08/2025  Page: 37</p>
--	--	--

## 12 Geometric Uncertainty

### 12.1 Description and impact analysis

---

The geometric uncertainty can be translated into a radiometric uncertainty by considering the difference between the radiometry integrated over the pixel at its nominal (expected) position and at its actual position.

The geometric uncertainty of Sentinel-2 images has been studied extensively, and depends on many elements such as:

- Focal plane calibration errors, depending mostly on detector module and spectral bands
- High-frequency errors (typically 5 Hz, across-track error oscillations)
- DEM error

For non-geometrically-refined images, one shall add systematic errors from the instrument geometric calibration and random pointing errors.

For geometrically refined images, systematic errors are coming from the geometric uncertainty of the Global Reference Image (GRI), while random errors are associated with refinement residuals.

All geolocation errors are propagated through the resampling process to L1C images.

### 12.2 Modelling

---

The radiometric impact of a geolocation uncertainty can be estimated from the norm of the image gradient (computed by finite differences).

For the RUT V1, we assume that the geolocation uncertainty of 1.5 m for refined images and 3 m for unrefined images.

### 12.3 Way forward


---

A further refinement would be to consider focal plane calibration residuals (between detectors and spectral bands).

### 12.4 Correlation

---

Geometric errors are highly correlated spatially, so their impact on radiometry is also correlated. They are also highly correlated between spectral bands. On the other hand, there is very little temporal and inter-satellite correlation. Only DEM and GRI error, which are small contributors, are temporally correlated.

	<p><b>OPT-MPC</b></p> <p><b>RUT error sources analysis</b></p>	<p>Ref.: OMPC.ACR.MEM.41  Issue: 1.0  Date: 01/08/2025  Page: 38</p>
--	--	--

## 13 L1C image quantization and compression error

### 13.1 Description and impact analysis

---

Before writing L1C images, the TOA radiance is converted to an integer using the quantization value ( $q = 10\ 000$ ) and compressed to a JP2000 image.

These steps should in principle introduce negligible errors. As far as quantization is concerned, the LSB at L1C ( $10^{-4}$ ) is negligible compared to the noise floor.

### 13.2 Synthesis and way forward

---

The L1C quantization noise is considered negligible.

While the L1C JP2000 compression noise may not be completely negligible in some cases, no attempt will be made to model this error. It is anticipated that new image formats (Zarr) will be introduced in the future, and the impact of L1C compression errors should be investigated again in this new context.

## 14 Conclusions


The following table provides a summary of the outcomes of the RUT error source analysis. As a follow-up of the study, we will propose additional consolidation work on the following terms:

- In-the-field straylight
- Polarization sensitivity

Orthorectification interpolation error. No satisfactory way forward was identified to model the following terms:


- Out-of-field straylight
- Spectral response non-uniformity

		Status RUT V1	Evolution in RUT V1
<b>L1B</b>	Instrument noise (+ quantization + dark noise)	modeled	parameterization revised
	in-the field straylight	not modeled	quantified on Moon images, way forward proposed
	Out of field straylight	modeled	parameterization revised
	cross-talk correction residual error	negligible	contribution removed, negligible
	polarization sensitivity	not modeled	way forward proposed
	on-board compression noise	negligible	quantified on ocean images, confirmed as negligible statistically
	dark signal correction residual error	negligible	unchanged
	non-linearity correction residual error	modeled	unchanged
	spectral response non-uniformity	not modeled	quantified on sample scenes
	L1B image quantization	negligible	unchanged
Radiometric calibration error	modeled	unchanged	
<b>L1C</b>	solar irradiance model error	negligible	unchanged
	Sun-satellite distance error	negligible	unchanged
	Cosine error	negligible	unchanged
	Orthorectification noise reduction	modeled	implemented
	orthorectification interpolation error	not modeled	way forward proposed
	Geolocation error	modeled	implemented
	L1C image quantization	negligible	unchanged

	<p><b>OPT-MPC</b></p> <p><b>RUT error sources analysis</b></p>	<p>Ref.: OMPC.ACR.MEM.41  Issue: 1.0  Date: 01/08/2025  Page: 40</p>
--	--	--

## 15 References

[RD1]	Gorroño, J.; Fomferra, N.; Peters, M.; Gascon, F.; Underwood, C.I.; Fox, N.P.; Kirches, G.; Brockmann, C. <b>A Radiometric Uncertainty Tool for the Sentinel 2 Mission</b> . Remote Sens. 2017, 9, 178. <a href="https://doi.org/10.3390/rs9020178">https://doi.org/10.3390/rs9020178</a>
[RD2]	Gorroño, J.; Banks, A.; Gascon, F.; Fox, N.P.; Underwood, C.I. <b>Novel techniques for the analysis of the TOA radiometric uncertainty</b> . Proc. SPIE 2016. <a href="https://doi.org/10.1117/12.2240391">https://doi.org/10.1117/12.2240391</a>
[RD3]	Javier Gorroño, Samuel Hunt, Tracy Scanlon, Andrew Banks, Nigel Fox, Emma Woolliams, Craig Underwood, Ferran Gascon, Marco Peters, Norman Fomferra, Yves Govaerts, Nicolas Lamquin & Veronique Bruniquel (2018) <b>Providing uncertainty estimates of the Sentinel-2 top-of-atmosphere measurements for radiometric validation activities</b> , European Journal of Remote Sensing, 51:1, 650-666, DOI: <a href="https://doi.org/10.1080/22797254.2018.1471739">10.1080/22797254.2018.1471739</a>
[RD4]	"Cross-talk simulation and related recommendations", J.F. Luce and S2MSI ESTEC, 24/01/2023.
[RD5]	OMPC.CS.MEM.06, "Specifications for IPF evolutions: Pixel-dependent cross-talk", i1.r0, 02/05/2022.
[RD6]	Sentinel-2 End-to-end mission, satellite and payload performance budgets a document (SY-25), Ref GS2.RP.ASF.MSI.00013, i10, 09/03/2015
[RD7]	Sentinel-2B End-to-end mission, satellite and payload performance budgets document (SY-15), REF GS2.RP.ASF.MSI.00234, i2, 24/05/2017
[RD8]	MSI Technical Budget report for C&D models (MS-18), GS2.RP.ASF.MSI.00247, i8, 26/06/2022
[RD9]	JCGM GUM-1:2023, Guide to the expression of uncertainty in measurement.
[RD10]	Javier Gorroño and Luis Guanter, "Assessing the radiometric impact of the Sentinel 2 orthorectification process", Proc. SPIE 11858, Sensors, Systems, and Next-Generation Satellites XXV, 118580W (12 September 2021); <a href="https://doi.org/10.1117/12.2603730">https://doi.org/10.1117/12.2603730</a>
[RD11]	Robert Ryan, "Landsat 8 OLI interpolation uncertainty estimation", JACIE uncertainty workshop, 07/05/2025, <a href="https://calval.cr.usgs.gov/apps/sites/default/files/jacie/recordings/JACIE2025-101.mp4">https://calval.cr.usgs.gov/apps/sites/default/files/jacie/recordings/JACIE2025-101.mp4</a>

	<p><b>OPT-MPC</b></p> <p><b>RUT error sources analysis</b></p>	<p>Ref.: OMPC.ACR.MEM.41  Issue: 1.0  Date: 01/08/2025  Page: 41</p>
--	--	--

[RD12]	OMPC.CS.TN016, "Sentinel-2C Impact of Spectral Response Differences", i1.0, 09/07/2025
--------	--

*End of document*